

# SC-Lane: Slope-aware and Consistent Road Height Estimation Framework for 3D Lane Detection

## Supplementary Material

### 1. Visualization of Input-LiDAR-Heightmap

To further elucidate the role of height information in our framework, we present an additional visualization of the Input-LiDAR-Heightmap in Fig. 1. This visualization illustrates how LiDAR-extracted height data is integrated into the model to enhance height estimation. Serving as a critical reference, the LiDAR-derived heightmap reinforces the structural understanding of road geometry and facilitates robust height prediction. By leveraging this information, our approach effectively aligns predicted heightmaps with real-world geometric constraints, contributing to a more structured and accurate BEV representation.

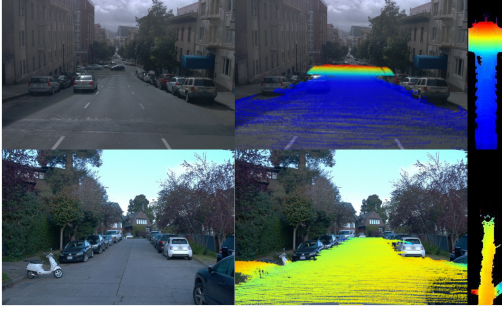


Figure 1. From left to right: Input image, LiDAR points from the ground projected onto the image, and the heightmap generated from these LiDAR points.

### 2. Activation of Slope-aware Adaptive Feature Weights

To validate the effectiveness of the Slope-aware Adaptive Feature module, we present a visualization of feature weight activations under different slope conditions in Fig. 2. This figure illustrates how our model dynamically adjusts slope-specific feature importance for adaptive and robust height estimation. The results demonstrate that our model selectively emphasizes relevant slope features while suppressing less informative regions, unlike fixed slope-based methods that apply uniform weighting. By dynamically modulating anchor blending based on the input image, the model enhances spatial awareness in height estimation, im-

proving structural consistency in BEV representations and ultimately boosting 3D lane detection accuracy.

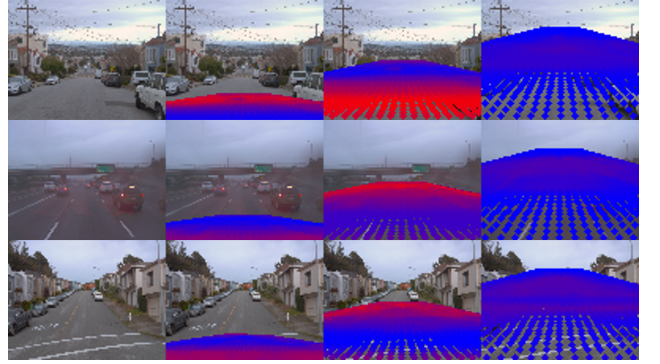


Figure 2. Visualization of Slope-aware Adaptive Feature Weight Activations. The first column represents the original input images. The second, third, and fourth columns show the projections of negative, zero, and positive slope anchors, respectively. The red regions indicate highly activated anchor weights, while the blue regions correspond to suppressed features.

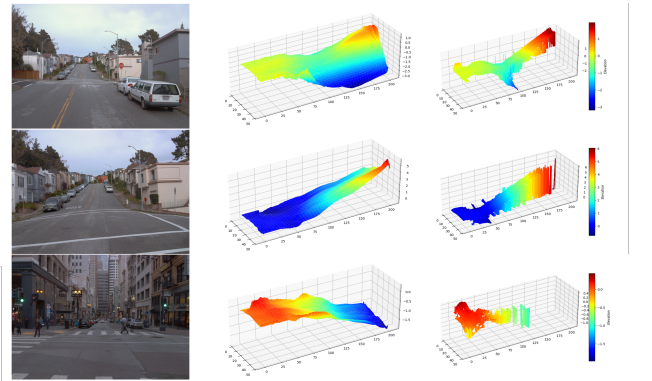


Figure 3. Comparison of predicted heightmaps with ground-truth heightmaps. From left to right: Input images, predicted heightmaps from our model, and ground-truth heightmaps.

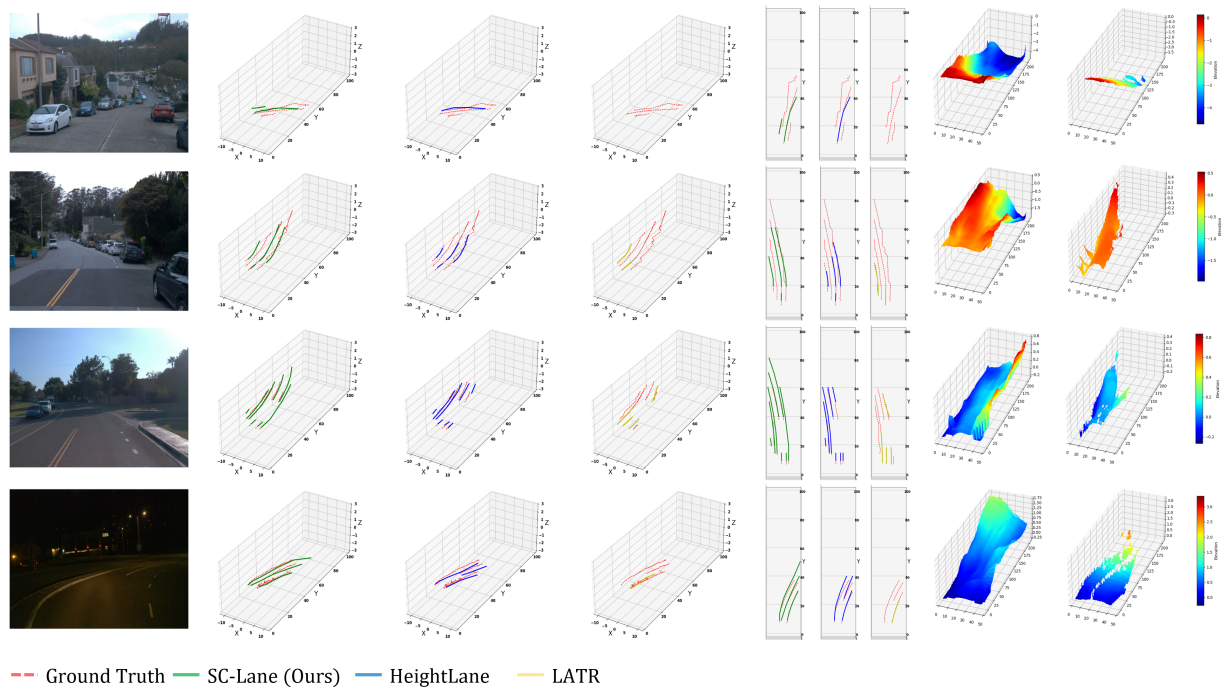


Figure 4. 3D visualization of lane height estimation. Similar to Figure 4 in the paper, but rendered in 3D to provide a more intuitive illustration of the predicted height variations. The visualization demonstrates that our method accurately captures lane elevation changes.

### 3. Additional Qualitative Results of Heightmap Estimation

To further demonstrate the effectiveness of our height estimation framework, we visualize the 3D lane detection results together with the corresponding heightmap predictions in Fig. 4. Moreover, Fig. 3 presents additional visualizations on challenging scenes with significant height variations, showing that our method accurately captures lane elevation changes even under complex conditions.

### 4. Additional Benchmark Results on the Apollo 3D Lane Dataset

To further assess the effectiveness of our approach, we conduct additional quantitative evaluations on the Apollo 3D Lane dataset. As presented in Tab. 1, we compare our method (SC-Lane) against existing state-of-the-art approaches, including BEVLaneDet [3], Anchor3DLane [1], and HeightLane [2]. The evaluation metrics include F-score, precision, recall, X-error (near and far), and Z-error (near and far).

SC-Lane achieves the highest overall F-score of 92.05%, surpassing the previous best method, HeightLane, which recorded 91.93%. In terms of recall, our method also attains the highest value of 94.47%, demonstrating its strong capa-

bility in detecting lanes comprehensively. While HeightLane slightly outperforms our method in precision (90.14% vs. 89.75%), SC-Lane achieves the best balance between precision and recall, leading to superior lane detection performance.

Regarding spatial localization errors, SC-Lane significantly reduces X-error (far) to 0.140, outperforming all other methods, including the second-best HeightLane (0.177).

### References

- [1] Shaofei Huang et al. Anchor3dlane: Learning to regress 3d anchors for monocular 3d lane detection. In *CVPR*, pages 17451–17460, 2023. 2, 3
- [2] Chaesong Park, Eunbin Seo, and Jongwoo Lim. Heightlane: Bev heightmap guided 3d lane detection. In *Proceedings of the Winter Conference on Applications of Computer Vision (WACV)*, pages 1692–1701, 2025. 2, 3
- [3] Ruihao Wang, Jian Qin, Kaiying Li, Yaochen Li, Dong Cao, and Jintao Xu. Bev-lanedet: An efficient 3d lane detection based on virtual camera via key-points. In *Proceedings of the IEEE/CVF Conference on Computer Vision and Pattern Recognition*, pages 1002–1011, 2023. 2, 3

Method	F-score	Precision	Recall	X-error(near)	X-error(far)	Z-error(near)	Z-error(far)
BevLaneDet[3]	89.69	86.58	93.02	0.134	0.184	0.053	<b>0.101</b>
Anchor3DLane[1]	87.33	87.31	87.35	<b>0.069</b>	0.289	<b>0.022</b>	0.183
HeightLane[2]	<u>91.93</u>	<b>90.14</b>	<u>93.79</u>	0.102	<u>0.177</u>	0.055	0.144
SC-Lane (ours)	<b>92.05</b>	<u>89.75</u>	<b>94.47</b>	<u>0.101</u>	<b>0.140</b>	<u>0.048</u>	<u>0.107</u>

Table 1. Quantitative results comparison by scenario on the Apollo 3D lane dataset. The best results for each scenario are highlighted in **bold** and second-best results are underlined.